# A Comparative Analysis of the Performance of COSMO and WRF Models in Quantitative Rainfall Prediction

Isaac Mugume, Charles Basalirwa, Daniel Waiswa, Mary Nsabagwa, Triphonia Jacob Ngailo, Joachim Reuder, Schättler Ulrich, Musa Semujju

*Abstract*—The Numerical weather prediction (NWP) models are considered powerful tools for guiding quantitative rainfall prediction. A couple of NWP models exist and are used at many operational weather prediction centers. This study considers two models namely the Consortium for Small–scale Modeling (COSMO) model and the Weather Research and Forecasting (WRF) model. It compares the models' ability to predict rainfall over Uganda for the period $21^{st}$ April 2013 to $10^{th}$ May 2013 using the root mean square (RMSE) and the mean error (ME). In comparing the performance of the models, this study assesses their ability to predict light rainfall events and extreme rainfall events. All the experiments used the default parameterization configurations and with same horizontal resolution (7 Km). The results show that COSMO model had a tendency of largely predicting no rain which explained its under–prediction. The COSMO model (RMSE: 14.16; ME: -5.91) presented a significantly (p = 0.014) higher magnitude of error compared to the WRF model (RMSE: 11.86; ME: -1.09). However the COSMO model (RMSE: 3.85; ME: 1.39) performed significantly (p = 0.003) better than the WRF model (RMSE: 8.14; ME: 5.30) in simulating light rainfall events. All the models under–predicted extreme rainfall events with the COSMO model (RMSE: 43.63; ME: -39.58) presenting significantly higher error magnitudes than the WRF model (RMSE: 35.14; ME: -26.95). This study recommends additional diagnosis of the models' treatment of deep convection over the tropics.

*Keywords*—Comparative performance, the COSMO model, the WRF model, light rainfall events, extreme rainfall events.

## I. INTRODUCTION

WEATHER predictions are required to guide decisions in a couple of sectors such as defense, agriculture, aviation and shipping among others [1]. The weather prediction process has always been a challenging problem as observed by Du et al. [2] and many others scholars. This challenge is normally caused by the chaotic nature

Isaac Mugume, Charles Basalirwa and Daniel Waiswa are Researchers in the department of Geography, Geoinformatics and Climatic Sciences at Makerere University, Uganda (e-mail: amooti23@gmail.com).

Mary Nsabagwa is a research in the department of networks, Makerere University, P. O. Box 7062, Kampala, Uganda.

Triphonia Jacob Ngailo is a research in the department of General Studies, Dar as Salaam Institute of Technology, P. O. Box 2958, Dar as salaam, Tanzania.

Joachim Reuder is a Professor in Geophysical Institute, University of Bergen, Allegaten 70, N–5007, Bergen, Norway.

Schättler Ulrich is an NWP Specialist at the Business Unit for Research and Development, Deutscher Wetterdienst (DWD), Frankfurter Strasse 135, 63067 Offenbach, Germany.

Musa Semujju is a weather Forecaster at the Directorate of Forecasting Services, Uganda National Meteorological Authority, P. O. Box 7025, Kampala, Uganda.

of the atmosphere and the incomplete knowledge of processes that govern the evolution of the atmosphere [3] which therefore introduces uncertainties in initial conditions. However objective methods of weather prediction are known and include the use of statistical weather prediction (SWP) methods and the use of numerical weather prediction (NWP) models [4].

The SWP methods rely on the relationships between the predictor and the predictand (Fig. 1) and include a couple of methods such as the use of linear regression, fuzzy logic, neural networks and many more. For example Paras et al. [1] used multiple linear regression to forecast rainfall, relative humidity and found a satisfactory prediction level. However, the SWP methods are limited by the quality of predictors, the suitable predictor–predictand relations and also require a long training predictor data set as explained by Grosjean et al. [5]. On the other hand, the NWP models consider the physical processes governing the atmosphere, representing them using governing equations and solving them numerically.
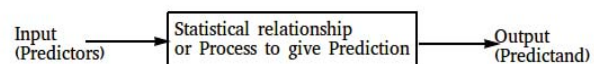


Fig. 1 Schematic illustration of the SWP method

This study uses the NWP models for quantitative rainfall forecast (QRF). QRF is considered a challenge over the Greater Horn of Africa, that includes Uganda, by Opijah et al. [6] because rainfall is a product of a complex chain of processes as explained by Böhme et al. [7] and Dierer et al. [8]. However, a study by Sokol & Rezacova [9] found that the NWP models at high horizontal resolution, as high as 1 Km can reproduce the precipitation fields comparable to the fields generated by meteorological radars. For this reason, Baldauf et al. [10] recognizes their role in producing severe weather guidance. The limitations observed in the predicted amount, location and evolution are caused by inappropriate rainfall triggering in the model [9] and the quality of the initial conditions [11].

One of the NWP models considered in this study is the COSMO model. It was formerly known as the Lokal Model and developed by meteorological services of Germany, Greece, Italy, Poland, Romania, Russia and Switzerland [10]

and they use it as the for operational weather prediction [8]. This model is a limited area non–hydrostatic model for forecasting operations on meso–$\beta$ (20–200 Km) and meso–$\gamma$ (2–20 Km) scales [10], [8]. A study by Baldauf et al. [10] using the COSMO model found it to satisfactorily simulate the convective events over Germany. Additionally, this model has been used in long–term rainfall validation studies by Böhme et al. [7] and we summarize the COSMO modeling system using Fig. 2 (a).
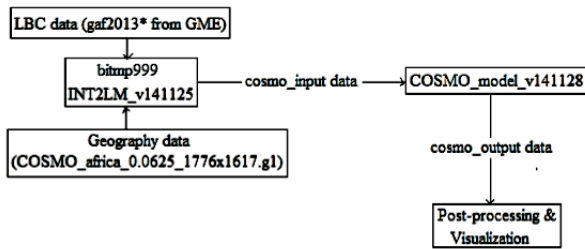


(a) The COSMO Model
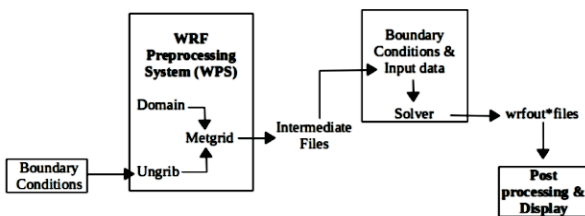


(b) The WRF Model

Fig. 2 Simplified illustration of the NWP models used

Another NWP model used is the Weather Research and Forecasting (WRF) model, which is a community model that has both advanced research core and a non–hydrostatic core suitable for research and operational weather prediction [12], [13]. A study by Xu et al. [14] found this model having the ability to simulate the diurnal patterns of rainfall. This model consists of the WRF Preprocessing System (WPS), the WRF-Variational (WRF-Var), the WRF-ARW solver and post-processing and visualization [15]. The dynamical core of the WRF model consists of non-hydrostatic dynamics, nesting capability, and several parameterization schemes [16] (Fig. 2 (b)). The WRF model is recommended for high resolution simulations by Mayor & Mesquita [17] and was developed for regional weather prediction and research [16]. It has been used in many NWP studies e.g. by Rajasekhar et al. [18], Krogsæter et al. [19] and many others.

Other NWP models for operational weather prediction are summarized in Table I. These models have varying horizontal resolution which is due to the available computing resources and production schedules [10], [11].

## II. Data and Methods

### A. Data Sources and Quality Control

The daily rainfall data were obtained from the Uganda National Meteorological Authority (UNMA) for 21 stations (Fig. 3) for the period 2000–2015. These data were used

TABLE I
Operational NWP models for Different Weather Prediction Centers. 'AROME' is Applications to Research on Operations at Mesoscale. JMA is the Japanese Meteorological Agency and UK MET is UK Meteorological Office

| NWP Model | Developer | Update | Resolution |
|---|---|---|---|
| Japanese Model | JMA | 8 h/day | 5 Km |
| Unified Model | UK MET | 6 h/day | 5 Km |
| AROME model | Meteo–France | 24 h | 2.5 Km |

to determine the extreme rainfall threshold values for the respective stations. The rainfall data for the period $21^{st}$ April to $10^{th}$ May 2013 was then used to assess the models' performance after first treating the rainfall data to quality control checks such as completeness and the possibility of unrealistic records like negative values.



Fig. 3 Map of Uganda showing the main study

The lateral boundary condition (LBC) data to initialize the NWP models were obtained from the German Weather Service (DWD) and the National Centers for Environmental Prediction (NCEP) final analysis [20] for the COSMO model and the WRF model respectively. The geographical data for the WRF model pre-processing were obtained from the U.S. Geological Survey while the geographical data for the COSMO model was obtained from DWD. The geographical data for COSMO was at a resolution of 7 km while the one for the WRF model was at 5 km.

### B. Experimental Design

The default physical parameterization schemes are used in all the models as recommended by the model developer but horizontal resolution in the WRF model is designed to match the default horizontal resolution of the COSMO model i.e. 7 Km resolution for Africa. A 12 hour spin–up time was allowed for the models to reduce spin-up errors. Additional configurations of the models used is presented in Sections II-B1 and II-B2 for the COSMO model and the WRF model respectively.

For a detailed assessment of the performance of the models, the case of $1^{st}$ May 2013 is used over Kasese region. On this day, the region experienced heavy rainfall that led to the bursting of rivers Nyamwamba and Mobuku and caused severe flooding; death of eight people and displacement of about 9,663 people. The flooding also caused damage to houses and bridges [21].

*1) COSMO Model Experiment Design:* The COSMO model runs are designed with 7 Km horizontal resolution single domain (Fig. 4 (a)) and having 50 vertical levels with a terrain–following height vertical coordinates and rotated horizontal geographical coordinate [8]. The model includes prognostic variables of horizontal and vertical components of wind, pressure perturbation, specific humidity, cloud water, temperature, and turbulent kinetic energy [10], [8]. The study employs the Tiedtke convective parameterization scheme and has triggers of both shallow and deep convection [22], a single moment microphysical scheme based on Lin et al. [23] having capability to predict rainwater, cloud water, cloud ice, graupel and snow and a radiation scheme based on the radiative transfer equation suggested by Ritter & Geleyn [24]. The rotated spherical coordinate system is used for the map projection and the model governing equations are solved on a staggered Arakawa C-grid [25], [10]. The model also employs Rayleigh damping in upper layers [8] and its dynamical core is based on the finite difference method [25], [8].

*2) WRF Model Experiment Design:* The WRF model version 3.8 experiment was designed with two domains (Fig. 4 (b)): the parent domain at a horizontal resolution of 35 Km and the nest at 7 Km horizontal resolution to enable performance comparison with the COSMO model at 7 Km horizontal resolution.

The WRF model used the staggered Arakawa C-grid; 30 vertical layers with model top fixed at 50 hPa; the terrain–following mass coordinate as vertical coordinate that allowed variation of vertical grid–spacing and the Runge-Kutta $2^{nd}$ order integration option. The default physical parameterization schemes are used which are the Kain–Fritsch convective scheme [26]; the WRF Single-Moment 3–class micro–physical scheme [27]; the Rapid Radiative Transfer Model as the longwave radiation scheme [28]; the Dudhia scheme as the shortwave radiation scheme [29]; the Noah Land Surface Model [30] and the Yonsei University scheme as the planetary boundary layer scheme [31]. Fig. 2 (b) illustrates the WRF modeling process used in the study.

*C. Methods*

The rainfall amount predicted by the model was computed as the grid–point area averaged precipitation values. The model output data were then compared with the station observed rainfall data to compute the root mean square error (A) & (1), the mean error (B) & (2) and the Students t-test (C) & (3) for statistical comparison of the difference in the means of the error magnitudes presented by the COSMO model and the WRF model. Additional assessment of the performance of the models is carried using the contingency table which is a categorical performance measures to assess the ability of the
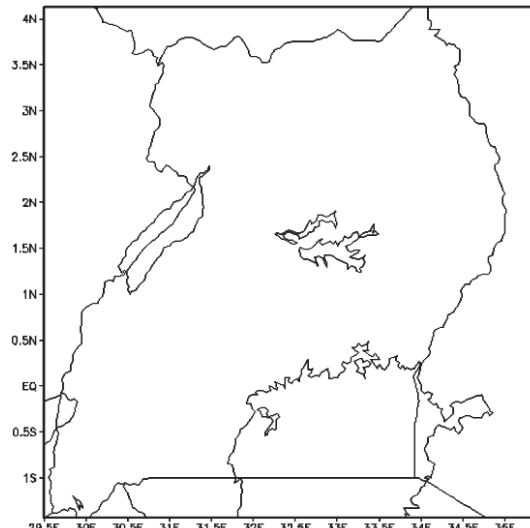


(a) The COSMO Model domain
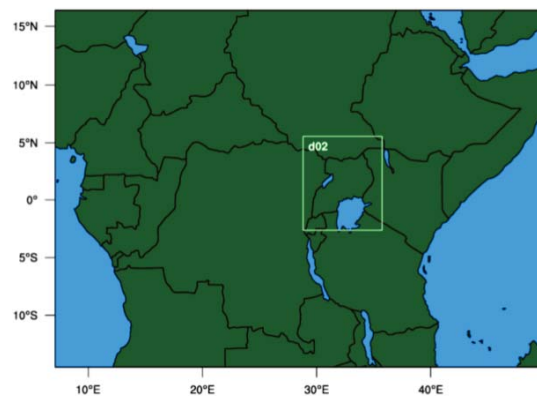


(b) The WRF Model domain

Fig. 4 Domain used in the study

models to predict occurrences of rainfall (i.e. occurrence of rain or no rain). The 2 x 2 contingency table is illustrated using Table II as presented by [32].

TABLE II
THE $2 \times 2$ CONTINGENCY TABLE

| | | Simulated | |
|---|---|---|---|
| | | Yes | No |
| Observed | Yes | HIT | MISS |
| | No | False Alarm (FAR) | Correct No |

III. RESULTS

*A. Overview of COSMO and WRF Model Performance*

The performance of the NWP models is presented using Table III for the root mean square error (RMSE) and the mean error (ME). The results shows that the RMSE of COSMO model ranges from 6.43 to 31.23 with a mean RMSE of 14.16 while the RMSE of WRF model ranges from 3.96 to 31.50 with a mean RMSE of 11.86. The ME results show that the ME of COSMO model ranges from -13.07 to 1.53 with a mean

ME of -5.91 and the ME for WRF model ranges from -7.88 to 7.15 with a mean ME of -1.09. Further investigation showed that for 16 out of 21 study location, the COSMO model presented a higher RMSE than the WRF model. Considering the magnitudes of the ME, the results show that for 17 out of 21 study locations, the COSMO model had a higher magnitude of ME than the WRF model. Additional analysis of the ME error results show that all the models generally underestimated rainfall but COSMO presented larger negative biases than WRF model.

TABLE III
PERFORMANCE RESULTS FOR COSMO AND WRF MODELS

| Station | COSMO Model | | WRF Model | |
|---|---|---|---|---|
| | RMSE | ME | RMSE | ME |
| Arua | 14.82 | -5.37 | 13.83 | -3.44 |
| Buginyanya | 13.69 | -9.26 | 18.2 | 7.15 |
| Bushenyi | 7.8 | -4.25 | 8.25 | -1.7 |
| Entebbe | 18.12 | -9.5 | 18.45 | -5.9 |
| Gulu | 6.43 | -2.26 | 4.96 | 2.02 |
| Jinja | 10.81 | 1.53 | 8.25 | 1.55 |
| Kabale | 6.98 | -4.17 | 4.03 | -0.86 |
| Kamenyamigo | 13.36 | -6.98 | 8.75 | -2.27 |
| Kasese | 9.99 | -3.94 | 9.8 | 1.04 |
| Kibanda | 10.78 | -6.8 | 6.81 | 3.62 |
| Kitgum | 18.82 | -13.07 | 12.6 | -5.79 |
| Kituza | 13.38 | 0.06 | 3.96 | -1.86 |
| Lira | 20.81 | -10.14 | 19.98 | -7.88 |
| Makerere | 20.16 | -5.23 | 11.95 | -6.01 |
| Masindi | 31.23 | -11.19 | 31.5 | -5.89 |
| Mbarara | 7.75 | -3.4 | 6.9 | 3.57 |
| Namulonge | 18.74 | -5.59 | 9.02 | -2.62 |
| Ntusi | 8.65 | -3.34 | 10.44 | 1.31 |
| Serere | 9.73 | -3.74 | 8.85 | 0.12 |
| Soroti | 16.13 | -7.71 | 16.12 | -2.11 |
| Tororo | 19.18 | -9.79 | 16.47 | -2.11 |
| Average | 14.16 | -5.91 | 11.86 | -1.09 |

Additional analysis for the light rainfall events (Table VI), defined as a rainfall event whose accumulated 24 hour rainfall amount is less than 1 mm, shows that the COSMO model had no rainfall on 23 light rainfall events out of 34. The COSMO model had an overall RMSE for light rainfall events of 3.85 and ME of 1.39. Further analysis of the COSMO models performance in predicting the extreme rainfall events (Table VII), defined by Ngailo et al. [33] as the rainfall events whose accumulated 24 hour rainfall amount is greater than the $95^{th}$ percentile showed that the COSMO model had an overall RMSE of 43.63 and ME of -39.58.

Additional analysis for light rainfall events (Table VI) shows that the WRF model generally overestimated light rainfall events over 21 cases out of 31 cases of light rainfall events. The WRF model presented an overall RMSE for light rainfall events of 8.14 and ME of 5.30. Further analysis of WRF models predictability of extreme rainfall events (Table VII) presented an overall RMSE of 35.14 and ME of -26.95. The under-prediction presented by the WRF model (ME = -26.95) was due to the under-predicted of 29 extreme rainfall events out of 35 events.

### B. The Case Study of $1^{st}$ May 2013

Spatial analysis of the performance of the COSMO and WRF models on $01^{st}$ May 2013 (Fig. 5) shows that COSMO model generally did not simulate rainfall over major regions of Uganda with exception of the Northeastern part of Lake Victoria Basin and some light rainfall over Kasese region (Fig. 5 (b)). The WRF model presented isolated rainfall cases over the Western Part of the country and heavy rainfall over the Eastern part of Uganda (Fig. 5 (g)).

Additional results are presented using Table IV and the results show that the COSMO model (ME: -7.03) presented significantly different mean error ($t = -2.246$; $p = 0.030$) compared to the WRF model (ME: 2.04). The COSMO model failed to simulate the heavy rainfall that pounded Kasese on $1^{st}$ May 2013 (i.e. 40.8 mm) while the WRF model under–predicted the rainfall (i.e. 7.5 mm)

The investigation of surface horizontal divergence showed that COSMO model (Fig. 6 (a)) largely gave positive horizontal divergence with a few areas having weak negative divergence (i.e. convergence) like over the Lake Victoria and Lake Kyoga compared to the surface horizontal divergence presented by the WRF model (Fig. 6 (b)). Both models presented a strong divergence over Kasese region with the WRF model presenting the strongest. Scientifically, the models should have simulated a low pressure region over Kasese but instead simulated a strong horizontal divergence. It is this failure of the models to simulate convection over Kasese region that probably explain their failure to simulate the heavy rains experienced over the region on $1^{st}$ May 2013.

Additional examination of the surface temperature (in deg. C) and mean sea level pressure (in hPa) presented using Fig. 7 as simulated by the models, showed that the COSMO model normally presented higher lake surface temperature compared to the lake temperatures simulated by the WRF model. Both models presented comparable surface temperatures over the case study area (Kasese region) and relatively similar sea level pressure simulations.

TABLE IV
PERFORMANCE RESULTS FOR COSMO AND WRF MODELS ON $01^{st}$ MAY 2013. 'OBS' IS OBSERVED RAINFALL IN MM; COSMO IS RAINFALL PREDICTED BY COSMO MODEL IN MM AND WRF IS RAINFALL PREDICTED BY WRF MODEL IN MM

| Station | Rainfall (mm) | | |
|---|---|---|---|
| | Obs | COSMO | WRF |
| Arua | 0 | 0 | 8.2 |
| Buginyanya | 10.3 | 0 | 12.7 |
| Bushenyi | 0 | 0 | 10.5 |
| Entebbe | 8.5 | 0 | 1.1 |
| Gulu | 1.4 | 0 | 10.3 |
| Jinja | 1.3 | 15.3 | 6.2 |
| Kabale | 6.3 | 0 | 8.2 |
| Kamenyamigo | 0 | 0 | 5.8 |
| Kasese | 40.8 | 0 | 7.5 |
| Kibanda | 2.1 | 0 | 10.9 |
| Kitgum | 41.5 | 0 | 29.8 |
| Kituza | 1.8 | 0.4 | 1.3 |
| Lira | 1.8 | 0 | 15.6 |
| Makerere | 5.4 | 0.1 | 0.9 |
| Masindi | 0 | 0 | 22 |
| Mbarara | 0 | 0 | 11.3 |
| Namulonge | 0 | 0.1 | 0 |
| Ntusi | 0 | 0 | 5.8 |
| Serere | 3.2 | 0 | 5.9 |
| Soroti | 4.7 | 0 | 14.2 |
| Tororo | 35 | 0.6 | 18.8 |

(a) COSMO 30/04

(b) COSMO 01/05

(d) COSMO 02/05

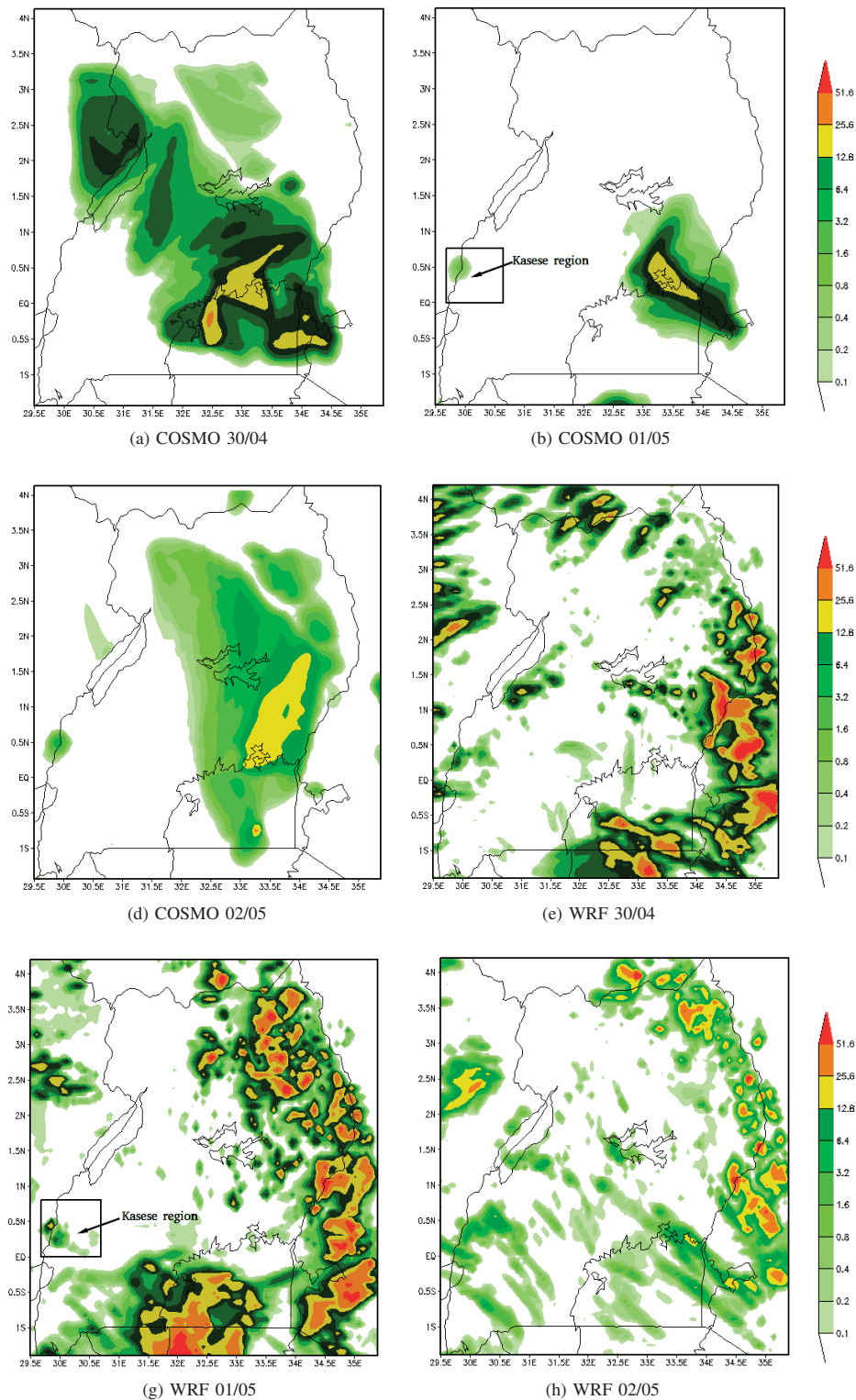(e) WRF 30/04

(g) WRF 01/05

(h) WRF 02/05

Fig. 5 Simulation of rainfall on $01^{st}$ May 2013 (i.e. 01/05). $30^{th}$ Apr. 2013 (i.e. 30/04) is used for spin–up and $02^{nd}$ May 2013 (i.e. 02/05) for post event analysis

## IV. Discussion

The Table III presented a comparison of the performance of the COSMO model and the WRF model. The RMSE results shows that for 16 out of 21 study location, the COSMO model
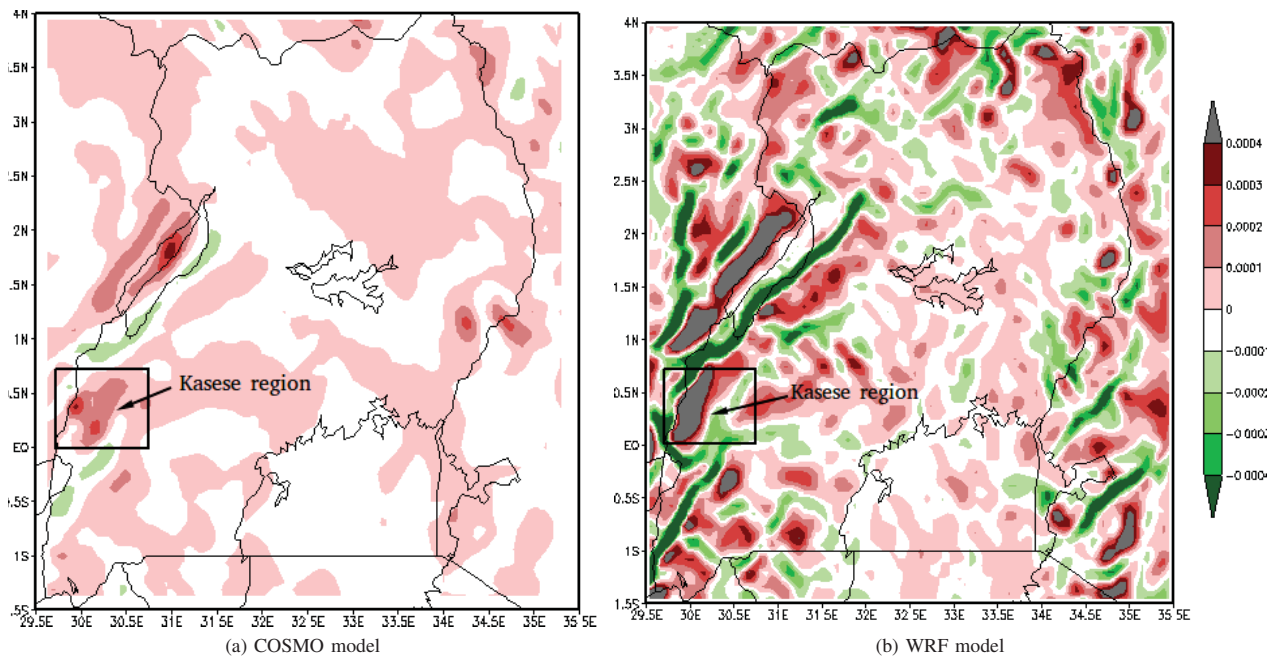
(a) COSMO model

(b) WRF model

Fig. 6 Surface horizontal divergence presented by the COSMO model (a) and the WRF model (b) on $01^{st}$ May 2013 (i.e. 01/05)
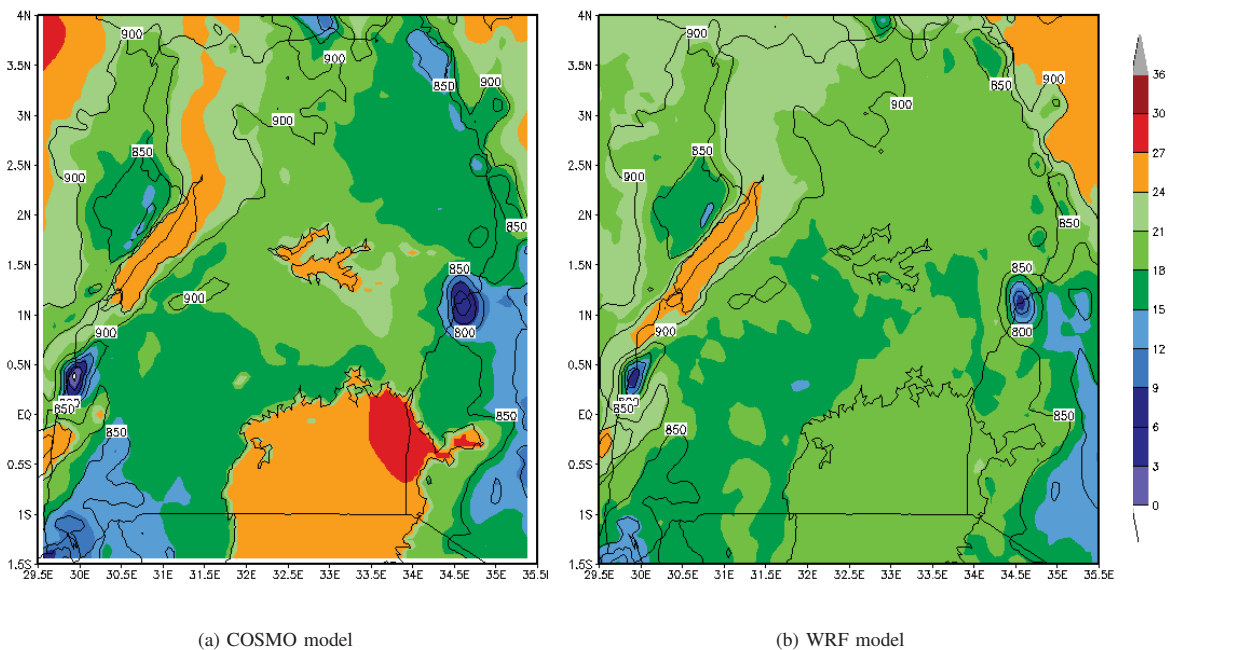


(a) COSMO model

(b) WRF model

Fig. 7 Surface temperature and mean sea level pressure presented by the COSMO model (a) and the WRF model (b) on $01^{st}$ May 2013 (i.e. 01/05)

presented a higher RMSE than the WRF model. Considering the magnitudes of the ME, the results show that for 17 out of 21 study locations, the COSMO model had a higher magnitude of ME than the WRF model. Additional analysis of the ME results show that all the models generally underestimated rainfall but COSMO presented larger negative biases than WRF model. This under-prediction of the models is also confirmed using the study case of $1^{st}$ May 2013 for Kasese region where all the models gave a high horizontal divergence (Fig. 6) compounded with weak surface temperatures (Fig. 7) which probably inhibited convective processes.

The comparative assessment of the COSMO model and the WRF model performance in predicting light rainfall events showed that the COSMO model presented a significantly

smaller RMSE than that of the WRF model (COSMO: 3.85 and WRF: 8.14). Further comparison of the mean errors presented by these models in predicting light rainfall events showed that the COSMO model presented a significantly (p = 0.003) smaller magnitude of ME compared to the WRF model (COSMO: 1.39 and WRF: 5.30). The weak performance of COSMO model against the WRF model was due to the failure of the COSMO model to simulate the rainfall events shown by MISS of 68.5% in Table V. The WRF model on the other hand presented a bigger magnitude of ME due to its high percentage of the false alarm of 72.9%.

TABLE V
PERFORMANCE MEASURES BASED ON THE CONTINGENCY TABLE

|                  | COSMO (%) | WRF (%) |
|------------------|-----------|---------|
| HIT              | 46.2      | 62.4    |
| FAR              | 31.3      | 72.9    |
| MISS             | 68.5      | 14.6    |
| Correct negative | 63.9      | 27.1    |

Additional investigation of the performance of the COSMO model in predicting the light rainfall events revealed that the COSMO model presented a smaller RMSE in predicting light rainfall events compared to the WRF model. This was caused by the COSMO model failure to predict rain on 23 out of 34 light rainfall events (Table VI) which was also revealed by a high percentage of the correct negative of 63.9% compared to 27.1% presented by the WRF model (Table V). These results show the under–performance of the COSMO model in simulating the light rainfall events which has also been reported in severe convective systems, complex orography and even with weak precipitation events by Böhme et al. (2011). Diagnostic studies by Dierer, et al. [8] and Crewell et al. [34] found that the COSMO model presented a dry humidity bias in the boundary layer and a wet humidity bias in middle troposphere over wet periods which, Dierer, et al. [8] suggested that it could probably explain the underestimation of rainfall. The predictability results of the light rainfall events further showed that the WRF model over–predicted the light rainfall events which was also found by Yang et al. [35] while evaluating the ability of WRF to simulate precipitation over the downstream area of the Yalong River Basin found in China.

The analysis of the COSMO and WRF models predictability of the extreme rainfall events showed that the COSMO model presented a significantly higher RMSE than the WRF model (COSMO: 43.63 and WRF: 35.14). A related study by Sokol & Rezacova [9] noted that whereas COSMO at a horizontal resolution of 2.8 Km provided the occurrence of the local storms in Czech Republic, the amounts of rainfall predicted were seriously underestimated and did not correspond to reality. Additional comparison of the errors presented by the COSMO and the WRF models further showed that the COSMO model presented significantly (p = 0.014) higher magnitude of error compared to the WRF model (COSMO: -39.58 and WRF: -26.95). The COSMO model missed many rainfall events including the extreme rainfall events (MISS: 68.5%) compared to the missed rainfall events presented by the WRF model of 14.6% (Table V).

## V. SUMMARY AND CONCLUSION

The study was aimed at comparing the performance of the COSMO model and the WRF model in the simulation of rainfall over the period $21^{st}$ April 2013 to $10^{th}$ May 2013. The results showed that the COSMO model presented a slight higher mean RMSE than that presented by the WRF model (RMSE of COSMO: 14.16 and RMSE of WRF: 11.86). The COSMO model also presented a higher magnitude of ME compared to the WRF model (ME of COSMO: -5.91 and ME of WRF: -1.09).

The COSMO model presented a smaller mean RMSE compared to the WRF model in simulating the light rainfall events (COSMO: 3.85 and WRF: 8.14). The COSMO model also presented a smaller magnitude of ME in simulating the light rainfall events compared to the WRF model (COSMO: 1.39 and WRF: 5.30). The results for predicting extreme rainfall events showed that the COSMO model has an overall RMSE of 43.63 compared to the RMSE presented by the WRF model of 35.14 and that both models under–predicted the extreme rainfall events including the case of Kasese on $01^{st}$ May 2013.

Additionally the COSMO model presented a significantly (p = 0.014) higher magnitude of mean error compared to the WRF model (COSMO: -39.58 and WRF: -26.95). The results generally show that the WRF model presents a better performance in simulating rainfall compared to the COSMO model over Uganda, the study region.

## APPENDIX

The study employed two performance measures i.e. the root mean square error (RMSE) and the mean error (ME).

### A. Root Mean Square Error

The RMSE is obtained from the square root of the mean square differences between predicted (i.e. $P$) and observed (i.e. $O$) when paired. It is computed mathematically as:

$$RMSE = \sqrt{\frac{1}{n} \sum_{i=1}^{n} [P_i - O_i]^2} \qquad (1)$$

### B. Mean Error

The ME is the mean of the differences (i.e $P_i - O_i$) which is computed as:

$$ME = \frac{1}{n} \sum_{i=1}^{n} [P_i - O_i] \qquad (2)$$

where $i$ is the $i^{th}$ data point ordered in time.

### C. The Student's t–Test

The t–test is a parametric test used to test whether there is a difference between the means of two univariate random variables [36]. The null hypothesis used in the study was that there is no difference between the RMSE of the two models. For the COSMO model and the WRF model with sample

TABLE VI
PERFORMANCE RESULTS OF COSMO AND WRF MODELS FOR THE
LIGHT RAINFALL EVENTS. 'OBS' IS OBSERVED LIGHT RAINFALL

| Station | Date | Light rainfall (mm) | | |
|---|---|---|---|---|
| | | Obs | COSMO | WRF |
| Buginyanya | 21. Apr. 2013 | 0.6 | 0 | 19.1 |
| Bushenyi | 28. Apr. 2013 | 0.2 | 0 | 0 |
| Entebbe | 30. Apr. 2013 | 0.5 | 11.2 | 9.7 |
| Gulu | 3. May. 2013 | 0.4 | 0.1 | 7.1 |
| Jinja | 9. May. 2013 | 0.3 | 13.3 | 0 |
| Kabale | 29. Apr. 2013 | 0.6 | 0 | 2.4 |
| Kasese | 25. Apr. 2013 | 0.8 | 0 | 0 |
| Kasese | 30. Apr. 2013 | 0.6 | 0 | 7.3 |
| Kasese | 2. May. 2013 | 0.9 | 0 | 0.7 |
| Kasese | 3. May. 2013 | 0.2 | 0 | 2.3 |
| Kamenyamigo | 22. Apr. 2013 | 0.3 | 0 | 7.2 |
| Kibanda | 26. Apr. 2013 | 0.2 | 0 | 7 |
| Kitgum | 23. Apr. 2013 | 0.3 | 0 | 0 |
| Kitgum | 2. May. 2013 | 0.5 | 0 | 9.4 |
| Lira | 22. Apr. 2013 | 0.2 | 0 | 0.1 |
| Makerere | 21. Apr. 2013 | 0.1 | 4.6 | 0 |
| Makerere | 22. Apr. 2013 | 0.3 | 0 | 4 |
| Makerere | 4. May. 2013 | 0.4 | 4.3 | 1.2 |
| Makerere | 9. May. 2013 | 0.4 | 2.3 | 0 |
| Makerere | 10. May. 2013 | 0.8 | 0 | 5.6 |
| Masindi | 24. Apr. 2013 | 0.4 | 0 | 0 |
| Mbarara | 28. Apr. 2013 | 0.1 | 0 | 6.9 |
| Mbarara | 7. May. 2013 | 0.3 | 0 | 11.8 |
| Ntusi | 23. Apr. 2013 | 0.2 | 0 | 0.3 |
| Ntusi | 3. May. 2013 | 0.4 | 0.1 | 0 |
| Ntusi | 5. May. 2013 | 0.5 | 0 | 5.4 |
| Serere | 3. May. 2013 | 0.3 | 10.7 | 0.3 |
| Serere | 5. May. 2013 | 0.2 | 0 | 6.3 |
| Serere | 8. May. 2013 | 0.4 | 4.1 | 9.7 |
| Soroti | 3. May. 2013 | 0.5 | 7.3 | 0.7 |
| Soroti | 5. May. 2013 | 0.6 | 0 | 16.1 |
| Tororo | 22. Apr. 2013 | 0.8 | 0 | 13.3 |
| Tororo | 27. Apr. 2013 | 0.2 | 0 | 21.9 |
| Tororo | 30. Apr. 2013 | 0.1 | 2.8 | 18 |

TABLE VII
PERFORMANCE RESULTS OF COSMO AND WRF MODELS FOR THE
EXTREME RAINFALL EVENTS. 'OBS' IS OBSERVED EXTREME RAINFALL

| Station | Date | Threshold | Light rainfall (mm) | | |
|---|---|---|---|---|---|
| | | | Obs | COSMO | WRF |
| Arua | 28. April 2013 | 19.9 | 50.1 | 0 | 0.6 |
| Arua | 8. May 2013 | 19.9 | 39.5 | 0 | 12.5 |
| Buginyanya | 29. April 2013 | 30.6 | 31.6 | 1.6 | 28.8 |
| Buginyanya | 9. May 2013 | 30.6 | 32.2 | 0.8 | 27.3 |
| Bushenyi | 2. May 2013 | 24.53 | 26.4 | 0 | 0 |
| Entebbe | 5. May 2013 | 35.95 | 39 | 0 | 6 |
| Gulu | 9. May 2013 | 20.54 | 26.1 | 1.4 | 18.4 |
| Kasese | 1. May 2013 | 18.5 | 40.8 | 0 | 7.5 |
| Kamenyamigo | 21. April 2013 | 15.73 | 40 | 0 | 16.3 |
| Kamenyamigo | 29. April 2013 | 15.73 | 27.5 | 0 | 8.2 |
| Kamenyamigo | 5. May 2013 | 15.73 | 27.8 | 0 | 8.6 |
| Kibanda | 5. May 2013 | 20.85 | 22.7 | 0 | 24.7 |
| Kibanda | 6. May 2013 | 20.85 | 29 | 0 | 30.1 |
| Kitgum | 21. April 2013 | 27.69 | 39 | 0 | 0.9 |
| Kitgum | 22. April 2013 | 27.69 | 37.6 | 0 | 21.4 |
| Kitgum | 1. May 2013 | 27.69 | 41.5 | 0 | 29.8 |
| Kitgum | 7. May 2013 | 27.69 | 28.4 | 0.2 | 7.7 |
| Kituza | 2. May 2013 | 34 | 34.3 | 1.4 | 31.2 |
| Lira | 5. May 2013 | 42.9 | 78 | 0 | 2.9 |
| Makerere | 28. April 2013 | 23.3 | 29.7 | 0 | 2.2 |
| Makerere | 29. April 2013 | 23.3 | 46.7 | 9.4 | 19 |
| Makerere | 2. May 2013 | 23.3 | 57.9 | 1.6 | 37.1 |
| Makerere | 6. May 2013 | 23.3 | 33.1 | 0 | 10.1 |
| Masindi | 25. April 2013 | 27.55 | 40.2 | 0 | 0 |
| Masindi | 27. April 2013 | 27.55 | 47.3 | 9.1 | 0.5 |
| Masindi | 6. May 2013 | 27.55 | 124.9 | 1 | 8.5 |
| Mbarara | 3. May 2013 | 27.08 | 30.5 | 0.1 | 20.4 |
| Namulonge | 21. April 2013 | 24.5 | 30.4 | 3.3 | 0 |
| Namulonge | 28. April 2013 | 24.5 | 40.5 | 0 | 22.4 |
| Namulonge | 30. April 2013 | 24.5 | 27 | 4.7 | 16.4 |
| Namulonge | 5. May 2013 | 24.5 | 50.5 | 0 | 41.1 |
| Ntusi | 4. May 2013 | 16.89 | 33.8 | 0 | 0.5 |
| Soroti | 2. May 2013 | 25.59 | 59.6 | 8.5 | 4 |
| Soroti | 4. May 2013 | 25.59 | 27.6 | 0 | 3 |
| Tororo | 4. May 2013 | 38.73 | 57.1 | 0 | 16.8 |

means $\overline{x}_1$ and $\overline{x}_2$ respectively, the Students $t$–test is defined by:

$$t = \frac{\overline{x}_1 - \overline{x}_2}{s_{12}\sqrt{\frac{1}{n_1} - \frac{1}{n_2}}} \qquad (3)$$

where $n_1$ and $n_2$ are the numbers of the variable of the COSMO model and the WRF model respectively and $s_{12}$ is the pooled standard deviation computed using:

$$s_{12}^2 = \frac{\sum_{i=1}^{n_1}(x_i - \overline{x}_1) + \sum_{i=1}^{n_2}(y_i - \overline{x}_2)}{n_1 + n_2 - 2} \qquad (4)$$

where $x$ and $y$ are the variables (i.e. the RMSE and ME) of the COSMO model and the WRF model respectively.

## ACKNOWLEDGMENTS

## REFERENCES

[1] M. Paras and M. Sanjay, "A simple weather forecasting model using mathematical regression.," *Indian Research Journal of Extension Education*, pp. 161–168, 2012.

[2] F. G. Du, W., X. Y. Hou, and W. Zhu, "A case study in flood fatality: Beijing July 2012 flood," 2013.

[3] D. J. Short Gianotti, B. T. Anderson, and G. D. Salvucci, "The potential predictability of precipitation occurrence, intensity, and seasonal totals over the continental United States.," *Journal of Climate*, pp. 6904–6918, 2014.

[4] I. Mugume, C. Basalirwa, D. Waiswa, J. Reuder, M. d. S. Mesquita, S. Tao, and T. J. Ngailo, "Comparison of parametric and nonparametric methods for analyzing the bias of a numerical model," *Modelling and Simulation in Engineering*, pp. 1–8, 2016.

[5] A. Grosjean and J. Kueny, "Statistical weather forecasting.," *Journal of Dynamics Systems, Measurement & Control.*, pp. 49–55, 1976.

[6] F. J. Opijah, "Application of the EMS-WRF Model in dekadal rainfall prediction over the GHA Region," *Africa Journal of Physical Sciences*, vol. 1, no. 1, pp. 2313–3317, 2014.

[7] T. Böhme, S. Stapelberge, T. Akkermans, S. Crewell, J. Fischer, T. Reinhardt, A. Seifert, C. Selbach, and N. V. Lipzig, "Long–term evaluation of COSMO Forecasting using combined observational data of the GOP period.," *Meteorologische Zeitschrift*, pp. 119–132, 2011.

[8] S. Dierer, A. Marco, S. Axel, A. Euripides, D. Rodica, G. Federico, M. Paola, M. Massimo, and S. Katarzyna, "Deficiencies in quantitative precipitation forecasts: Sensitivity studies using the COSMO model.," *Meteorologische Zeitschrift*, vol. 18, no. 6, pp. 631–645, 2009.

[9] Z. Sokol and D. Rezacova, "Assimilation of radar reflectivity into the LM COSMO Model with a high horizontal resolution.," *Meteorological Applications*, vol. 13, pp. 317–330, 2006.

[10] M. Baldauf, A. Seifert, J. Förstner, D. Majewski, and M. Raschendorfer, "Operational convective–scale numerical weather prediction with the COSMO Model: Description and sensitivities.," *Monthly Weather Review*, vol. 139, pp. 3887–3905, 2011.

[11] T. T. Warner, *Numerical weather and climate prediction*. Cambridge University Press., 2010.

[12] S. Cai and H. Yu, "Analysis of different Weather Research and Forecasting Radiation schemes impact on the numerical simulation of a typical mesoscale convective weather in china.," *Journal of Atmospheric and Solar-Terrestrial Physics*, vol. 80, pp. 68–72, 2012.

[13] B. Xie, J. C. Fung, A. Chan, and A. Lau, "Evaluation of nonlocal and local planetary boundary layer schemes in the WRF Model.," *Journal of Geophysical Research: Atmospheres,*, vol. 117, 2012.

[14] G. Xu, Y. Xie, C. Cui, Z. Zhou, W. Li, and J. Xu, "Sensitivity of the summer precipitation simulated with WRF Model to Planetary Boundary Layer Parameterization over the Tibetan Plateau and its Downstream Areas.," *Journal of Geology and Geophysics*, vol. 5, no. 4, pp. 1–11, 2012.

[15] W. Wang, C. Bruyere, M. Duda, J. Dudhia, D. Gill, H. C. Lin, and J. Mandel, "Arw version 3 modeling system users guide.," tech. rep., National Center for Atmospheric Research: Mesoscale and Microscale Meteorology Division., www2.mmm.ucar.edu, 2015.

[16] C. Pennelly, G. Reuter, and T. Flesch, "Verification of the WRF Model for simulating heavy precipitation in Alberta.," *Atmospheric Research*, vol. 135, no. 136, pp. 172–192, 2014.

[17] Y. G. Mayor and M. D. S. Mesquita, "Numerical simulations of the 1 May 2012 deep convection event over Cuba: sensitivity to cumulus and microphysical schemes in a high–resolution model.," *Advances in Meteorology*, vol. 2015, pp. 1–11, 2015.

[18] M. Rajasekhar, T. Sreeshna, M. Rajeevan, and S. Ramakrishna, "Prediction of severe thunderstorms over Sriharikota Island by using the WRF–ARW Operational model," *SPIE 50Asia-Pacific Remote Sensing,*, vol. 2016, pp. 988214–988214, 2016.

[19] O. Krogsæter and J. Reuder, "Validation of boundary layer parameterization schemes in the Weather Research and Forecasting model under the aspect of offshore wind energy applicationspart I: Average wind speed and wind shear," *Wind Energy*, vol. 18, no. 5, pp. 769–782, 2015.

[20] E. Kalnay, M. Kanamitsu, R. Kistler, W. Collins, D. Deaven, L. Gandin, M. Iredell, S. Saha, G. White, J. Woollen, *et al.*, "The ncep/ncar 40-year reanalysis project," *Bulletin of the American meteorological Society*, vol. 77, no. 3, pp. 437–471, 1996.

[21] I. Mugume, D. Waiswa, M. Mesquita, J. Reuder, C. Basalirwa, Y. Bamutaze, R. Twinomuhangi, F. Tumwine, J. Sansa-Otim, T. Jacob Ngailo, and G. Ayesiga, "Assessing the Performance of WRF Model in Simulating Rainfall over Western Uganda.," *Journal of Climatology and Weather Forecasting*, vol. 5, no. 1, pp. 1–9, 2017.

[22] M. Tiedtke, "A comprehensive mass flux scheme for cumulus parameterization in large–scale models.," *Monthly Weather Review*, vol. 117, no. 8, pp. 1779–1800, 1989.

[23] Y. L. Lin, R. D. Farley, and H. D. Orville, "Bulk parameterization of the snow field in a cloud model.," *Journal of Climate and Applied Meteorology*, vol. 22, no. 6, pp. 1065–1092, 1983.

[24] B. Ritter and J. F. Geleyn, "A comprehensive radiation scheme for numerical weather prediction models with potential applications in climate simulations.," *Monthly Weather Review,*, vol. 120, no. 2, pp. 303–325, 1992.

[25] S. Brdar, M. Baldauf, A. Dedner, and R. Klöfkorn, "Comparison of dynamical cores for NWP Models: Comparison of COSMO and Dune.," vol. 27, no. 3–4, pp. 453–472, 2013.

[26] J. S. Kain, "The Kain–Fritsch Convective Parameterization: An update.," *Journal of Applied Meteorology,*, vol. 43, pp. 170–181, 2003.

[27] S. Y. Hong, J. Dudhia, and S. H. Chen, "A revised approach to ice microphysical processes for the bulk parameterization of clouds and precipitation.," *Monthly Weather Review,*, vol. 132, no. 1, pp. 103–120, 2004.

[28] S. A. Clough, M. W. Shephard, E. J. Mlawer, J. S. Delamere, M. J. Iacono, K. Cady-Pereira, ..., and P. D. Brown, "Atmospheric radiative transfer modeling: a summary of the aer codes.," vol. 91, no. 2, pp. 233–244, 2005.

[29] J. Dudhia, "Numerical study of convection observed during the winter monsoon experiment using a mesoscale two–dimensional model.," *Journal of the Atmospheric Sciences*, vol. 46, no. 20, pp. 3077–3107, 1989.

[30] G. Y. Niu, Z. L. Yang, K. E. Mitchell, F. Chen, M. B. Ek, M. Barlage, ..., and M. Tewari, "The Community Noah Land Surface Model with Multiparameterization Options (Noah MP): Model Description and Evaluation with Local–Scale Measurements.," *Journal of Geophysical Research: Atmospheres,*, vol. 116, 2011.

[31] X. M. Hu, J. W. Nielsen-Gammon, and F. Zhang, "Evaluation of three Planetary Boundary Layer Schemes in The WRF Model.," *Journal of Applied Meteorology and Climatology*, vol. 49, no. 9, pp. 1831–1844, 2010.

[32] J. Liu, M. Bray, and D. Han, "Sensitivity of the weather research and forecasting (wrf) model to downscaling ratios and storm types in rainfall simulation," *Hydrological Processes*, vol. 26, no. 20, pp. 3012–3031, 2012.

[33] T. J. Ngailo, N. Shaban, J. Reuder, E. Rutalebwa, and I. Mugume, "Non Homogeneous Poisson Process Modelling of Seasonal Extreme Rainfall Events in Tanzania," *International Journal of Science and Research (IJSR)*, vol. 5, no. 10, pp. 2319–7064, 2016.

[34] S. Crewell, M. Mech, T. Reinhardt, C. Selbach, H.-D. Betz, E. Brocard, G. Dick, E. OConnors, J. Fischer, T. Hanisch, T. Hauf, A. Huenerbein, L. Delobbe, A. Mathes, H. Peters, H. Wernli, M. Weigner, and V. Wulfmeyer, "The General Observation Period 2007 within the Priority Program on Quantitative Precipitation Forecasting: Concepts and First Results.," *Meteorologische Zeitschrift*, vol. 17, pp. 849–866., 2008.

[35] T.-H. Yang, S.-C. Yang, J.-Y. Ho, G.-F. Lin, G.-D. Hwang, and C.-S. Lee, "Flash flood warnings using the ensemble precipitation forecasting technique: a case study on forecasting floods in taiwan caused by typhoons.," *Journal of Hydrology*, vol. 520, pp. 367–378, 2015.

[36] v. S. Hans and F. W. Zwiers, *Statistical Analysis in Climate Research*. Cambridge University Press, 2003.